Adenosine inhibits voltage-dependent Ca^{2+} currents in rat dissociated supraoptic neurones via A_1 receptors

Jun Noguchi and Hiroshi Yamashita

Department of Physiology, School of Medicine, University of Occupational and Environmental Health, Kitakyushu 807-8555, Japan

(Received 8 November 1999; accepted after revision 14 April 2000)

1. The modulation of voltage-dependent Ca^{2+} currents (I_{Ca}) by adenosine was investigated in magnocellular neurones acutely dissociated from the rat hypothalamic supraoptic nucleus (SON) by using the whole-cell patch-clamp technique.

2. Adenosine dose dependently and reversibly inhibited I_{Ca} elicited by depolarizing voltage steps from a holding potential of −80 mV to potentials ranging from −30 to +20 mV. The mean (± S.E.M.) maximum inhibition rate was 36·1 ± 4·1 % ($n = 6$) at −20 mV and the EC_{50} was $9{\cdot}8 \times 10^{-7}$ M ($n = 6$).

3. The inhibition of I_{Ca} by adenosine was completely reversed by the selective A_1 receptor antagonist 8-cyclopentyl theophylline (CPT), and was mimicked by the selective A_1 receptor agonist N^6-cyclohexyladenosine (CHA).

4. The inhibition by CHA was strongly reduced when I_{Ca} was inhibited by ω-conotoxin GVIA, a blocker of N-type Ca^{2+} channels.

5. The adenosine-induced inhibition of I_{Ca} was largely reversed by a depolarizing prepulse to +150 mV for 100 ms, which is known to reverse the inhibition of Ca^{2+} channels mediated by G-protein $\beta\gamma$ subunits.

6. The adenosine receptor-mediated inhibition of I_{Ca} was not abolished by intracellularly applied preactivated pertussis toxin (PTX).

7. Using immunohistochemistry, $G_z\alpha$-like immunoreactivity (a PTX-resistant inhibitory G-protein) was observed throughout the SON.

8. These results suggest that adenosine modulates the neuronal activity of SON neurones by inhibiting N-type voltage-dependent Ca^{2+} channels via A_1 receptors which are coupled to PTX-resistant G-proteins.

Magnocellular neurones in the hypothalamic supraoptic nucleus (SON) synthesize arginine vasopressin and oxytocin. These peptides are released into the systemic circulation from axon terminals located in the neurohypophysis, and the released amount is closely related to the electrical activity of SON neurones (Bourque, 1991; Leng & Brown, 1997). This electrical activity is regulated by humoral factors and synaptic neurotransmitters/neuromodulators, such as glutamate and γ-aminobutyric acid, various peptides and other physiological active substances including purinergic agents (Hatton, 1990; Brann, 1995; Shibuya *et al.* 1999).

In various regions of the mammalian central nervous system (CNS), adenosine is well known to act as a neurotransmitter/neuromodulator (Fredholm & Dunwiddie, 1988). Adenosine modulates neural excitability and acts as a neural sleep factor in basal forebrain and mesopontine cholinergic neurones (Rainnie *et al.* 1994), as an endogenous anticonvulsant in the hippocampus and amygdala (Dragunow, 1988), as a modulator of LTP in the hippocampus (de Mendonća & Ribeiro, 1994) and as a neuroprotective agent in the hippocampus (Dragunow & Faull, 1988). At present, classification of adenosine receptors is based on both their protein sequences and their affinity for a variety of ligands (Fredholm *et al.* 1994). Four subtypes of adenosine receptor have been cloned and pharmacologically characterized: A_1, A_{2a}, A_{2b} and A_3 receptors. A_1 and A_3 receptors are thought to be coupled to G_i and/or G_o proteins, while A_{2a} and A_{2b} are coupled to G_s protein (Fredholm *et al.* 1994; Palmer & Stiles, 1995). The various effects of adenosine on neuronal activity are thought to occur through the modulation of Ca^{2+} channels and/or K^+ channels (Fredholm & Dunwiddie, 1988; Fredholm *et al.* 1994; Palmer & Stiles, 1995). It has been reported that adenosine modulates voltage-dependent calcium channels (VDCCs) in the postsynaptic membrane of many different

neuronal cell types, such as hippocampus, brainstem and superior cervical ganglion (Mogul *et al.* 1993; Zhu & Ikeda, 1993; Umemiya & Berger, 1994; Fleming & Mogul, 1997).

Previous binding, immunohistochemistal and *in situ* hybridization studies have reported that the level of the various adenosine receptors in rat brain hypothalamus is very low. Only the A_1 receptor subtype has been detected in the SON using both *in situ* hybridization and immunohistochemistry (Reppert *et al.* 1991; Rivkees *et al.* 1995). In addition, no reports on the effects of adenosine in SON neurones have been published as yet.

In SON neurones, Ca^{2+} entry through VDCCs plays a crucial role in the generation and/or maintenance of their action potential firing patterns, which are closely linked to arginine vasopressin and oxytocin secretion. For example modulation of VDCCs alters the bursting properties these cells, the action potential plateau and the width of the action potential (Bourque & Renaud, 1985; Andrew, 1987).

In the present study, we investigated the expression of adenosine receptors in the SON using reverse transcription-polymerase chain reaction (RT-PCR) techniques. In addition, we studied the effects of adenosine on the VDCCs in acutely dissociated SON neurones using the whole-cell patch-clamp technique.

METHODS

Preparation of SON slices

Young adult male Wistar rats at 5–8 weeks of age (125–250 g) were used in all experiments. All animal procedures in these studies were carried out in accordance with the guidelines on the use and care of laboraory animals as set out by the Physiological Society of Japan and approved by the animal care committee at this institution. For preparation of SON slices, rats were first stunned by a blow to the neck and then immediately decapitated. The brain was quickly removed and cooled in a bathing solution at 4 °C for approximately 1 min. The bathing solution contained (mM): NaCl, 124; KCl, 5; $MgSO_4$, 1·3; KH_2PO_4, 1·24; $CaCl_2$, 2; $NaHCO_3$, 25·9; and glucose, 10. The osmolality, as determined with a One-Ten osmometer (Fiske Associates, Norwood, USA), was 300–310 mosmol kg^{-1}. This bathing solution was continuously oxygenated and equilibrated with a mixture of 95% O_2–5% CO_2. A block containing the hypothalamus was cut from the brain and glued to the stage of a vibratome-type slicer (DSK-2000; DOSAKA EM Co., Ltd, Kyoto, Japan), and then immersed in 4 °C bathing solution. Coronal slices of 300 μm thickness containing the SON were cut from this brain block and then carefully trimmed around the SON using a circular micropunch (i.d. 1·0 mm) and fine scissors so as not to include any extra-SON tissue. For RT-PCR, these trimmed slices were immediately frozen by transferring them into liquid nitrogen. For electrical recordings, these trimmed slices were pre-incubated in the bathing solution at room temperature (23–25 °C) for at least 1 h and then transferred to a digestion solution for dissociation of individual SON neurones.

RT-PCR

Total RNA was extracted from the SON slices, using the RNeasy mini kit (Qiagen, Hilden, Germany). RT-PCR was then performed with a thermal cycler (Perkin-Elmer, CA, USA) using a RT-PCR kit (Toyobo, Osaka, Japan). The specificities of the four independent sense and antisense primer pairs for A_1, A_{2a}, A_{2b} and A_3 receptors used in the present study have previously been described (Dixon *et al.* 1996). Reverse transcription of the total RNA (0·5 μg) from each slice was performed in a final volume of 20 μl using random primers and Moloney murine leukaemia virus reverse transcriptase with the RT-PCR kit. PCR was performed with a RT-PCR buffer containing 1 μM primers, 1 mM each deoxynucleotide triphosphate, 2·5 U recombinant Taq DNA polymerase and each transcribed cDNA, in a final volume of 50 μl. Single-stranded cDNA products were denatured and subjected to PCR amplification (30 cycles). Each PCR cycle consisted of denaturation at 94 °C for 45 s, annealing at 64 °C for 50 s and finally extension at 72 °C for 65 s. Primers for a house-keeping gene, glyceraldehyde 3-phosphate dehydrogenase (G3PDH), were used as an internal standard. The PCR products were separated by electrophoresis on a 2% agarose gel and visualized by ethidium bromide staining.

Acute dissociation of SON magnocellular neurones

After incubation at room temperature for at least 1 h, the trimmed slices were transferred into a digestion solution for 90 min at 28 °C. This digestion solution was the same as the bathing solution except that it also contained trypsin (0·1 mg ml^{-1}, Sigma type XI). The slices were then transferred into a bathing solution which contained trypsin inhibitor (1 mg ml^{-1}; Nacalai Tesque, Kyoto, Japan) for 10 min at 28 °C. They were then placed back into the bathing solution for up to 8 h until use. Individual trimmed slices were transferred to a culture dish and then mechanically dissociated by trituration with fire-polished glass pipettes (tip i.d. ranging from 250 to 650 μm) in a standard recording solution (described below), continuously oxygenated with humidified 100% O_2. The dissociated neurones were left for at least 5 min before recordings were commenced to enable them to adhere to the bottom of the culture dish.

Recording solutions

Standard recording solution (Hepes-buffered solution; HBS) contained (mM): NaCl, 140; KCl, 5; $MgCl_2$, 1; $CaCl_2$, 2; Hepes, 10; and glucose, 11·1. The osmolality was 300–310 mosmol kg^{-1} and pH was adjusted to 7·4 with NaOH. HBS was continuously oxygenated with 100% O_2 throughout the experiments.

Ca^{2+} current (I_{Ca}) recording solution was HBS with 0·001 mM tetrodotoxin (TTX), and Mg^{2+} was omitted. The pH and osmolality were the same as for standard HBS. I_{Ca} recording solution was also continuously oxygenated with 100% O_2. The pipette solution used for I_{Ca} measurements was designed to block K^+ currents and contained (mM): tetraethylammonium hydrochloride (TEA-Cl), 100; 4-aminopyridine (4-AP), 5; $MgCl_2$, 1; $CaCl_2$, 1; EGTA, 10; Hepes, 10; Mg-ATP, 2; creatine phosphate di-Tris salt, 20; and Na_2-GTP, 0·3. The osmolality was 280–290 mosmol kg^{-1} and pH was adjusted to 7·2 with Tris base. I_{Ca} was pharmacologically isolated by inclusion of TTX in the I_{Ca} recording solution to block Na^+ currents. K^+ currents were also blocked by inclusion of TEA-Cl and 4-AP in the pipette solution. Leak and capacitative currents were cancelled by off-line subtraction of Ni^+ (100 μM)- and Cd^{2+} (200 μM)-insensitive currents. 'Rundown' of I_{Ca} throughout the 80 min recording period was effectively reduced by using an ATP-regenerating system. Pertussis toxin (PTX) was intracellularly applied using a modified method of Kakehata *et al.* (1993). PTX was preactivated by adding it to pipette solution containing dithiothreitol (5 mM) and then left for 30 min at 37 °C. It was then diluted in additional pipette solution containing β-nicotinamide adenine dinucleotide (NAD, 5 mM) before being added to the pipette. The final concentration of PTX was 1 μg ml^{-1}.

Table 1. Individual adenosine receptor primers for RT-PCR

Primer	Source	Position (bp)	Sequence (5′ to 3′)	Predicted length (bp)
A_1	M64299	630–649 (S)	CTC CAT TCT GGC TCT GCT CG	207
		836–818 (AS)	ACA CTG CCG TTG GCT CTC C	
A_{2a}	L08102	407–423 (S)	CCA TGC TGG GCT GGA ACA	150
		556–536 (AS)	GAA GGG GCA GTA ACA CGA ACG	
A_{2b}	M91466	139–156 (S)	TGG CGC TGG AGC TGG TTA	160
		298–281 (AS)	GCA AAG GGG ATG GCG AAG	
A_3	M94152	238–256 (S)	AGA AGC TAG GTC CAC TGG C	665
		902–880 (AS)	GCA CAT GAT AAC CAG GGG GAT GA	

Sources are described by the GenBank accession number. S, sense; AS, antisense.

Whole-cell patch-clamp recordings

Dissociated neurones were perfused with the standard recording solution at a flow of 1·5 ml min^{-1}. The solution in the dish was kept at a constant volume by a low pressure aspiration system. Magnocellular neurones were identified using an upright microscope (Nikon, Tokyo, Japan). Only whole-cell tight-seal (1–5 GΩ) patch-clamp recordings were made from neurones which had the typical morphological appearance of magnocellular SON neurones: a large soma of > 15 μm diameter. Over 96% of the neurones selected by the above criteria were thought to be neurosecretory cells (Oliet & Bourque, 1992). Patch-clamp electrodes were made from glass capillaries (GD-1·5, Narishige, Tokyo, Japan) using a horizontal pipette puller (P-87, Sutter Instrument Co., Novoto, USA). They had a final resistance of between 6 and 8 MΩ when filled with the pipette solution. All electrophysiological recordings were carried out at room temperature (23–25 °C). Recording of membrane currents was generally delayed for 5–10 min after membrane rupture until the I_{Ca} reached a steady level; however, the effects of PTX on the adenosine-induced inhibition of VDCCs were examined shortly after membrane rupture because PTX is known to show an effect within a few minutes (Kakehata *et al.* 1993). Currents were filtered at 5 kHz and recorded using a patch-clamp amplifier (Axopatch 200A, Axon Instruments Inc.), and were digitized at 10 kHz using pCLAMP software (version 6.0.3; Axon Instruments Inc.) for subsequent off-line analysis. The standard recording solution was switched to the I_{Ca} recording solution immediately after successful membrane rupture using a peristaltic pump. The time required for the complete change of I_{Ca} recording solution and addition of drugs was estimated to be a few seconds.

Pharmacological agents

Adenosine, N^6-cyclohexyladenosine (CHA), N^6-[2-(3,5-dimethoxyphenyl)-9-ethyl]adenosine (DPMA), N^6-[2-(4-aminophenyl)ethyl]-adenosine (APNEA), 8-cyclopentyl-3,7-dihydro-1,3-dimethyl-1H-purine-2,6-dione (CPT) and 3,7-dimethyl-1-propargylxanthine (DMPX) were purchased from Research Biochemicals International (MA, USA). Trypsin, NAD and creatine phosphate di-Tris salt were from Sigma. TTX was from Sankyo Co., Ltd (Tokyo, Japan). All of the peptide toxin Ca^{2+} channel blockers were from Peptide Institute (Osaka, Japan). PTX was from Seikagaku Co., Ltd (Tokyo, Japan). All other chemicals were from Nacalai Tesque.

Analysis

Data were analysed using AxoGraph software (version 3.6; Axon Instruments Inc.). I_{Ca} was measured between 3 and 8 ms after the depolarizing voltage steps and averaged for further analysis. The magnitude of I_{Ca} inhibition was expressed as percentage inhibition of the control current, which was the averaged current measured just before application of drugs and after complete recovery from the drug effects. Dose–response curves were fitted with the empirical Hill equation using the least-squares method (AxoGraph, version 3·6).

All data shown represent the mean ± S.E.M. Statistical comparisons were performed using non-parametric tests (Mann-Whitney U test). $P < 0{\cdot}05$ was regarded as a statistically significant difference.

Immunohistochemistry

Rats were deeply anaesthetized by intraperitoneal injection of sodium pentobarbital (50 mg kg^{-1}), and then perfused transcardially with 100 ml of 0·1 M phosphate buffer (pH 7·4) containing heparin (500 U (500 ml)$^{-1}$) and 150 ml of fixative containing 4% paraformaldehyde and 0·2% picric acid in 0·1 M phosphate buffer.

After postfixation and cryoprotection in 20% sucrose, 40 μm thick serial sections were cut using a microtome and processed as free-floating sections. The primary G_z α subunit antibody was a rabbit anti-G_z α subunit, N-terminal (amino acids 3–18) antiserum (Calbiochem-Novabiochem Corporation, San Diego, CA, USA), diluted 1:1000 in 0·1 M phosphate-buffered saline (PBS) containing 0·3% Triton X-100. After treatment with 1% hydrogen peroxidase for 1 h at room temperature, the sections were incubated with the primary antibody solution at 4 °C for 5 days. The avidin–biotin peroxidase complex (Vectastain ABC kit, Vector Laboratories Inc., Burlingame, USA) in the sections was visualized with 0·02% 3,3′-diaminobenzidine (DAB) for 20–30 min. This experiment was then repeated twice, independently.

Control sections were incubated with the same diluted G_z α subunit antiserum after it had been preincubated with synthetic peptide corresponding to the N-terminal sequence (amino acids 3–18) of the G_z α subunit (10^{-4} M) (Yanaihara Institute Inc., Shizuoka, Japan).

RESULTS

RT-PCR analysis of adenosine receptors in the SON

To identify subtypes of adenosine receptor in the SON, RT-PCR using four pairs of primers was performed (Table 1). In contrast to previous *in situ* hybridization

studies, we observed that mRNAs for A_1, A_{2a}, A_{2b} and A_3 receptors were expressed in the SON (Fig. 1), although the expression level of the A_3 subtype was very low.

Effects of adenosine on voltage-dependent Ca^{2+} currents

To investigate the effects of adenosine on VDCCs in SON neurones, Ca^{2+} currents were elicited from a holding potential (V_h) of −80 mV to depolarized test potentials (ranging from −60 to +50 mV) for 50 ms. Figure 2*A* shows a representative I_{Ca} and also the time course of I_{Ca} inhibition by adenosine. Mean values between 3 and 8 ms (●) and between 24 and 34 ms (○) at a test potential of −20 mV were used to evaluate I_{Ca} amplitude. Application of 10^{-5} M adenosine reversibly inhibited evoked I_{Ca} in all cells tested ($n = 6$) with a rapid onset and a relatively slow recovery. Figure 2*B* shows superimposed current tracings before, during and after application of 10^{-5} M adenosine. In addition to inhibiting the steady-state current, adenosine also slowed the activation of I_{Ca} ('kinetic slowing'). Such characteristics of I_{Ca} inhibition by adenosine were observed in all six SON neurones from which we recorded. Figure 2*C*1 shows the averaged 3–8 ms current–voltage relationships obtained from these six SON neurones.

Figure 2*C*2 shows summary data for the voltage dependence of the inhibition of I_{Ca} by adenosine. Adenosine significantly inhibited I_{Ca} at voltages between −30 and +20 mV with a peak inhibition at −20 mV. The mean maximum inhibition at −20 mV was 36·1 ± 4·1 % ($n = 6$).

The dose–response relationship of the adenosine-induced inhibition of I_{Ca} was studied using voltage steps to −20 mV from a holding potential of −80 mV. Figure 3*A* demonstrates that the inhibition of I_{Ca} by adenosine was dose dependent. This concentration dependence of the adenosine block was fitted with the empirical Hill equation by the least-squares method (Fig. 3*B*). Inhibition of I_{Ca} by the A_1 receptor agonist CHA showed a similar dose dependence but CHA was more potent by about one order of magnitude. The half-maximal concentration (EC_{50}) for the inhibition of I_{Ca} by adenosine was $1{\cdot}0 \times 10^{-6}$ M ($n = 6$) and by CHA was $5{\cdot}8 \times 10^{-8}$ M ($n = 5$) (Fig. 3*B*). Maximum inhibition was observed at 10^{-5} M (32·2 ± 0·9 %) in the case of adenosine, and at 10^{-6} M (35·0 ± 2·0 %) in the case of CHA. Recently, it was reported that in the SON, adenosine inhibits presynaptic neurotransmitter release via an A_1 receptor (Oliet & Poulain, 1999). IC_{50} values were reported as $12{\cdot}7 \times 10^{-6}$ M for inhibition of IPSCs and $12{\cdot}8 \times 10^{-6}$ M for inhibition of EPSCs. Our present results indicate that the postsynaptic response to adenosine in the SON appeared at a concentration about one order of magnitude lower than that for the presynaptic response. In both cases, the adenosine-induced response was reversed by CPT, the A_1-selective antagonist. These results suggest that adenosine affects both pre- and postsynaptic A_1 receptors in the SON.

Pharmacological analysis of adenosine receptor subtypes

To analyse which adenosine receptor subtypes mediated the inhibition of I_{Ca} in the SON, we used the following relatively selective adenosine receptor ligands: CHA (A_1 agonist), DPMA (A_2 agonist), APNEA (A_3 agonist), CPT (A_1 antagonist) and DMPX (A_2 antagonist). The effects of the agonists and antagonists were evaluated independently, and at concentrations that exhibited a maximum response (CHA, 10^{-6} M; DPMA, 10^{-6} M; APNEA, 10^{-6} M; CPT, 10^{-6} M; and DMPX, 10^{-5} M).

The selective A_1 receptor antagonist CPT completely reversed adenosine-induced inhibition of I_{Ca} without enhancement, whereas the A_2 receptor antagonist DMPX caused only a partial reversal of adenosine-induced inhibition. The effects of these antagonists on the CHA-induced inhibition were similar to the effects on adenosine-induced inhibition (Fig. 4*A* and *B*). These results suggest that adenosine

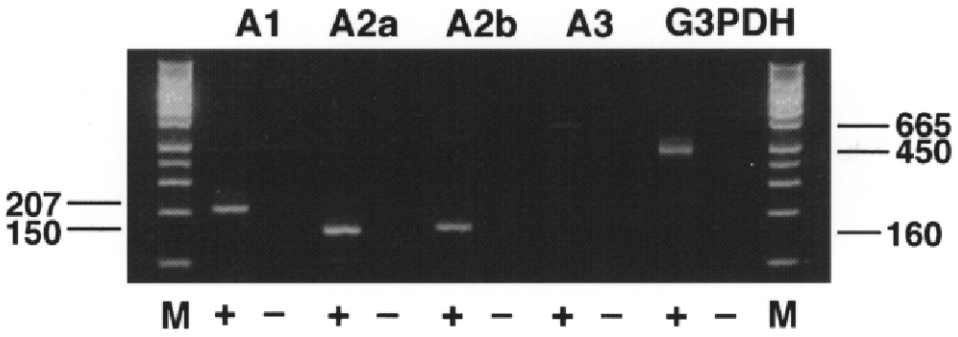

Figure 1. RT-PCR analysis of adenosine receptor mRNAs expressed in the rat SON

Total RNA from rat SON was reverse transcribed (+) or not (−), then amplified by PCR with each of the primer pairs described in Table 1. Primers for G3PDH were used as an internal control and generated a 450 bp fragment. Amplification products were electrophoresed on a 2% agarose gel and visualized by ethidium bromide staining. Lane M, Hi-Lo DNA ladder marker (Avetech, Tokyo, Japan). When PCR from each sample was performed without prior reverse transcription, there was no amplification product, indicating that the bands appearing on the gel were not derived from genomic DNA. The sizes of the bands are given in base pairs.

induces inhibition of I_{Ca} through the A_1 receptor. The relatively selective A_2 agonist DPMA, however, also inhibited I_{Ca}, but the percentage inhibition by DPMA was smaller than that induced by adenosine or CHA (adenosine, $34{\cdot}9 \pm 4{\cdot}3\%$, $n = 4$; CHA, $37{\cdot}1 \pm 7{\cdot}3\%$, $n = 6$ *vs.* DPMA, $10{\cdot}4 \pm 1{\cdot}4\%$, $n = 7$; $P < 0{\cdot}05$). Inhibition of I_{Ca} by DPMA was completely reversed by CPT but also by the A_2 antagonist DMPX (Fig. 4*C*). These results also suggest that DPMA-induced inhibition of I_{Ca} is likely to be mediated through the A_1 receptor. The relatively selective A_3 agonist APNEA inhibited I_{Ca} but the inhibition was almost completely reversed by CPT and DMPX (Fig. 4*C*). These results suggest that adenosine-induced inhibition of VDCCs in SON neurones occurred mainly though the A_1 adenosine receptor, although there was possibly a small A_2 contribution, and furthermore demonstrate the lack of specificity of these ligands.

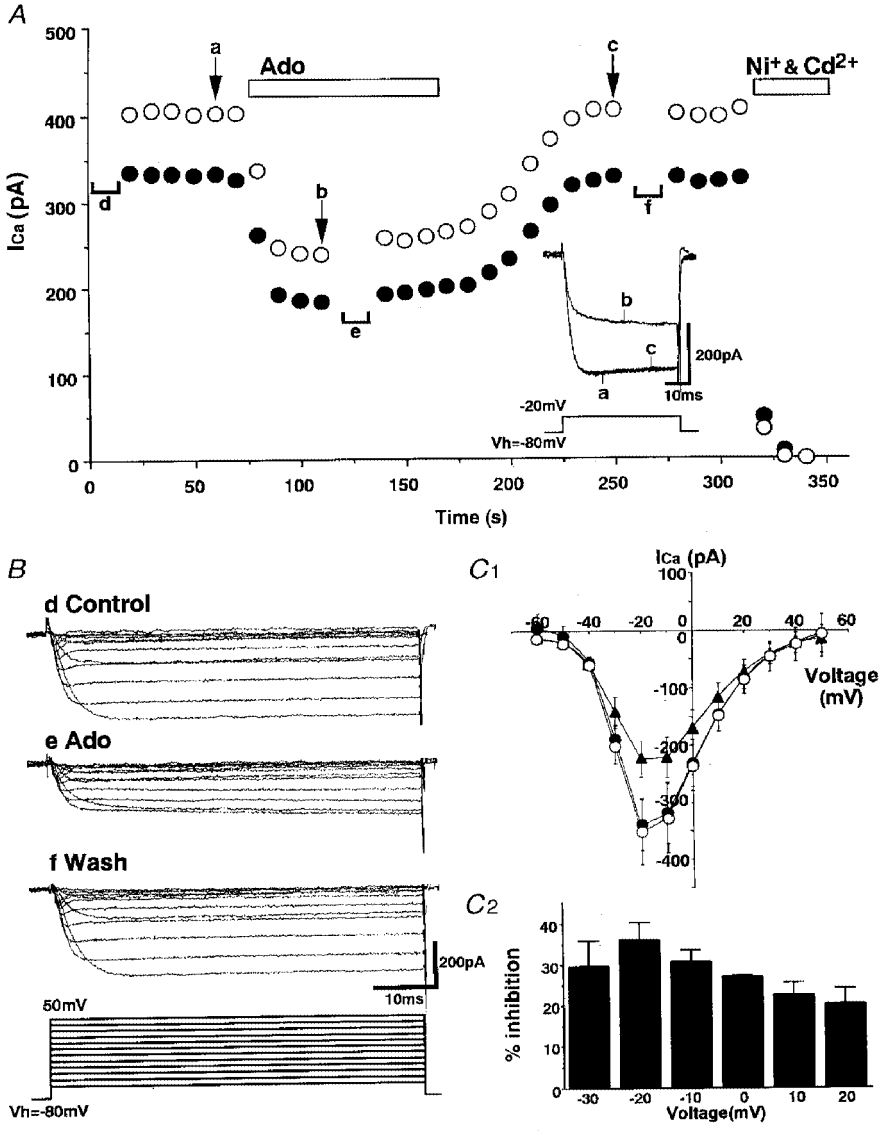

Figure 2. Inhibition of I_{Ca} by adenosine in SON magnocellular neurones

A, a representative experiment illustrating the time course of adenosine (Ado, 10^{-5} M)-induced inhibition of I_{Ca}. Leak currents were cancelled by subtraction of the current remaining after application of Ni^+ (10^{-4} M) and Cd^{2+} (2×10^{-4} M). I_{Ca} values between 3 and 8 ms (●), and between 24 and 34 ms (○), after the beginning of the test pulse were averaged. Inset, superimposed I_{Ca} traces obtained at times *a*, *b* and *c*. *B*, representative I_{Ca} traces in response to voltage steps (to between −60 mV and +50 mV) from $V_h = -80$ mV before (Control), during and after (Wash) application of 10^{-5} M adenosine. The traces were obtained at times *d*, *e* and *f* in *A*. *C*1, summary of the current–voltage relationship of I_{Ca} before (●), during (▲) and after (○) application of 10^{-5} M adenosine. I_{Ca} amplitude was calculated as the averaged current between 3 and 8 ms after the beginning of the test pulse ($n = 6$). Error bars indicate S.E.M. *C*2, voltage dependence of the adenosine (10^{-5} M)-induced inhibition of I_{Ca}. Data are shown as the mean ± S.E.M. of values obtained from six neurones.

Effects of blockers of Ca^{2+} channels on inhibition by A_1 agonist

To detect which types of VDCC contributed to the component of I_{Ca} that was inhibited by adenosine, we used the selective Ca^{2+} channel blockers ω-conotoxin-GVIA (ω-CTx-GVIA; N-type), ω-agatoxin IVA (ω-Aga-IVA) plus ω-conotoxin MVIIC (ω-CTx-MVIIC) (P/Q-type), and nifedipine (L-type). Both the contribution of different subtypes of VDCC to the total calcium influx and the relative percentage of CHA-induced inhibition of each subtype were measured.

Figure 5*A* shows a representative example trace illustrating the experimental protocol and the I_{Ca} classification used in the present study. The small component of the I_{Ca} that reversed upon washout of the irreversible toxin-blockers ω-CTx-GVIA, ω-Aga-IVA and ω-CTx-MVIIC was considered to represent L-type current (α_{1D} subunit) as described by Brinbaumer *et al.* (1994). The percentage of the total I_{Ca} characterized by these blockers was: N-type, 27·0 ± 3·4%; P/Q-type, 15·0 ± 3·9%; L-type, 16·6 ± 4·1%; and the residual (R-type) current was 41·3 ± 4·0% ($n = 4$; Fig. 5*B*, outer circle). The percentage inhibition (expressed as percentage of the total I_{Ca}) of each I_{Ca} subtype by CHA

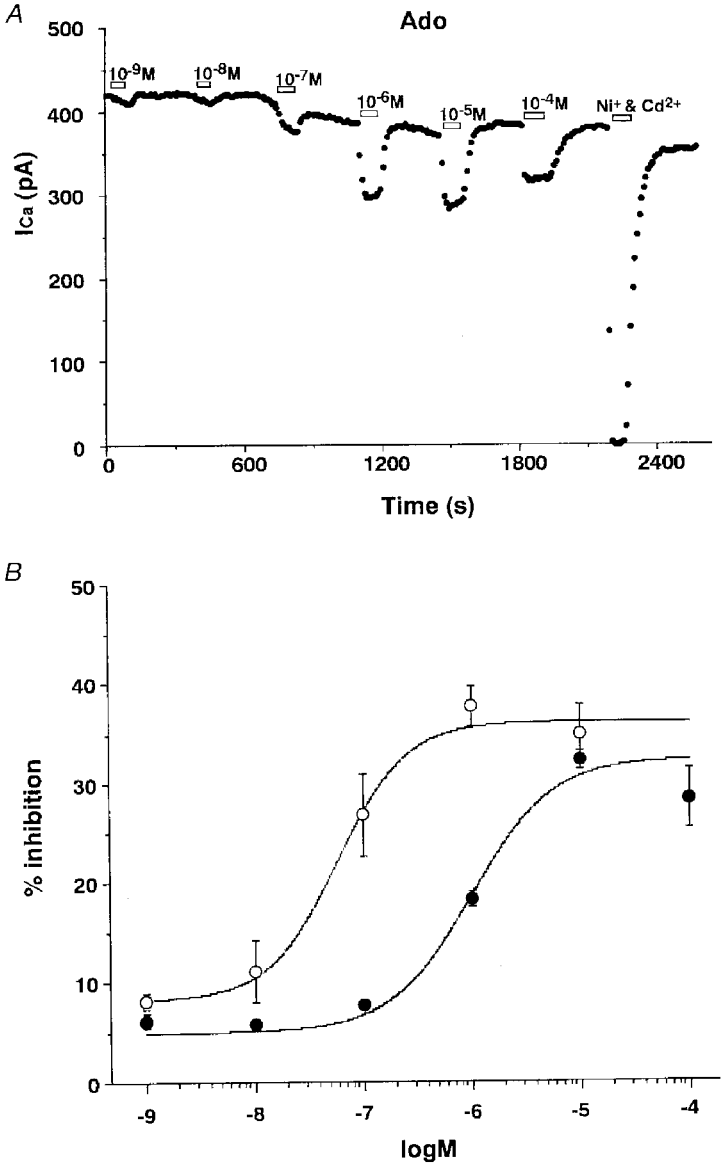

Figure 3. Dose–response relationship of adenosine-induced inhibition of I_{Ca}

A, a representative experiment illustrating the time course of the dose dependence of inhibition of I_{Ca} by adenosine (Ado, 10^{-9} to 10^{-4} M). *B*, dose–response curves of I_{Ca} inhibition induced by adenosine (●) and CHA (○). Curves represent the Hill fits to the mean data using the least-squares method. The Hill coefficients obtained from the curves were 1·17 (adenosine) and 1·36 (CHA). Data are shown as the mean ± S.E.M. of values obtained from seven (10^{-9} to 10^{-5} M) and six (10^{-4} M) experiments in adenosine, and from five (10^{-9} to 10^{-5} M) experiments in CHA.

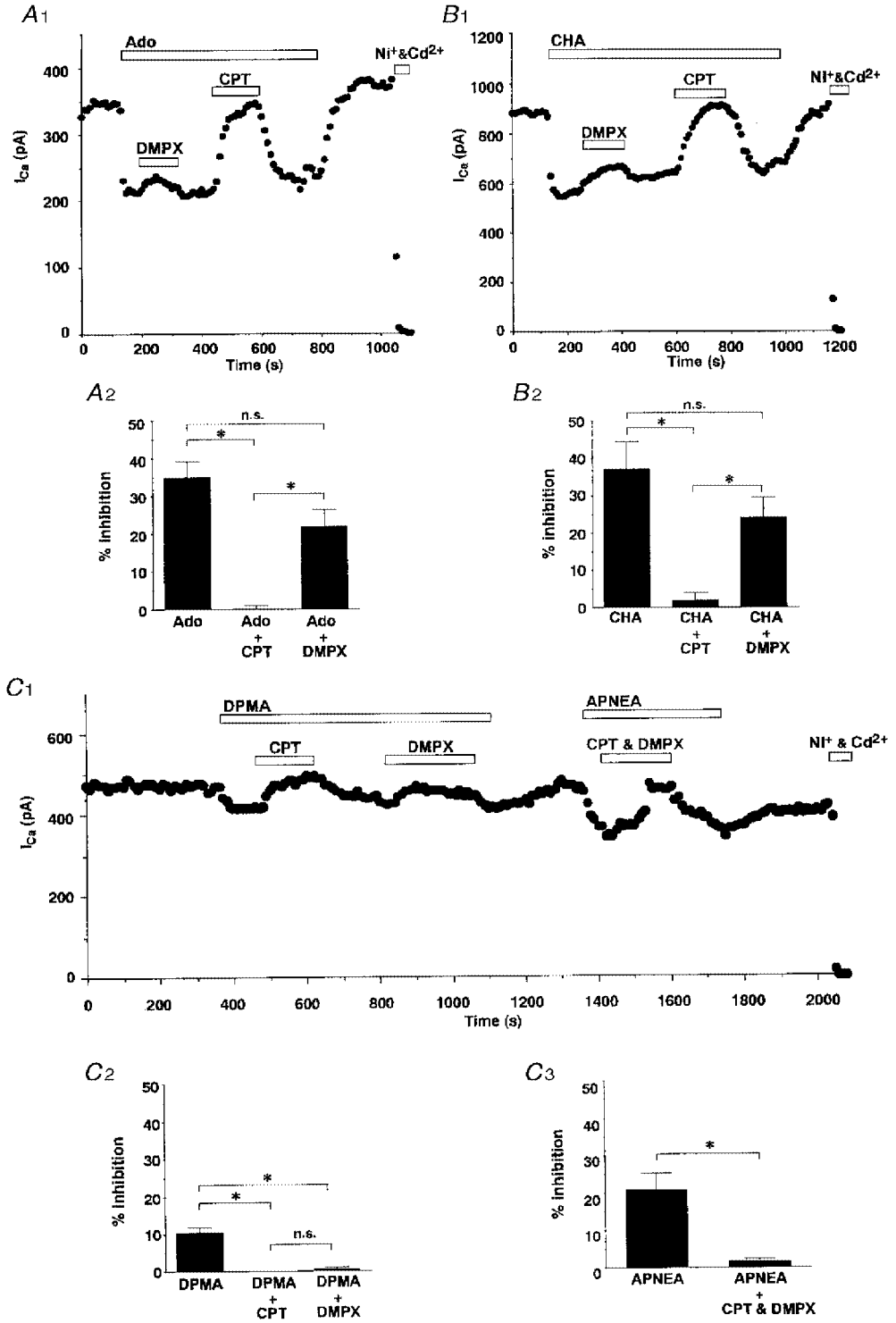

Figure 4. Pharmacological characterization of the receptor subtype involved in adenosine-induced I_{Ca} inhibition

*A*1 and *B*1, representative experiments illustrating the effects of the A_1 antagonist CPT (10^{-6} M) and the A_2 antagonist DMPX (10^{-5} M) on 10^{-6} M adenosine (*A*1)- and 10^{-6} M CHA (*B*2)-induced I_{Ca} inhibition. *A*2 and *B*2, summary of the effects of CPT and DMPX on 10^{-6} M adenosine (*A*2)- and 10^{-6} M CHA (*B*2)-induced I_{Ca} inhibition (adenosine, $n = 4$; CHA, $n = 5$). *C*1, representative experiments illustrating the effects of CPT and DMPX on DPMA (10^{-6} M)- and APNEA (10^{-6} M)-induced I_{Ca} inhibition. *C*2, summary of the effects of CPT and DMPX on DPMA-induced I_{Ca} inhibition ($n = 7$). *C*3, summary of the effects of CPT and DMPX on APNEA-induced I_{Ca} inhibition ($n = 4$). $^*P < 0{\cdot}05$; n.s., not significant.

was: N-type, 21·1 ± 4·2%; P/Q-type, 4·5 ± 1·8%; L-type, 4·8 ± 0·9%; and R-type, 6·6 ± 1·5% ($n = 4$; Fig. 5*B*, inner circle). Thus the relative contribution of each subtype of I_{Ca} for the inhibition by CHA were calculated as: N-type, 54·7%; P/Q-type, 12·0%; L-type, 14·9%; and R-type, 17·4% ($n = 4$; Fig. 5*C*). These results indicate that N-type Ca^{2+} channels are the main contributors in to the inhibition of I_{Ca} by A_1 receptor activation.

Effects of prepulse and dialysis with preactivated PTX on adenosine-induced inhibition of VDCCs

The rapid onset, in the order of seconds, for the inhibition of I_{Ca} by adenosine indicates that the response might be mediated by a membrane-delimited mechanism. It is well established that a large depolarizing prepulse reverses the inhibition of I_{Ca} by the membrane-delimited action of G-protein $\beta\gamma$ subunits (Ikeda, 1996; Herlitze *et al.* 1996;

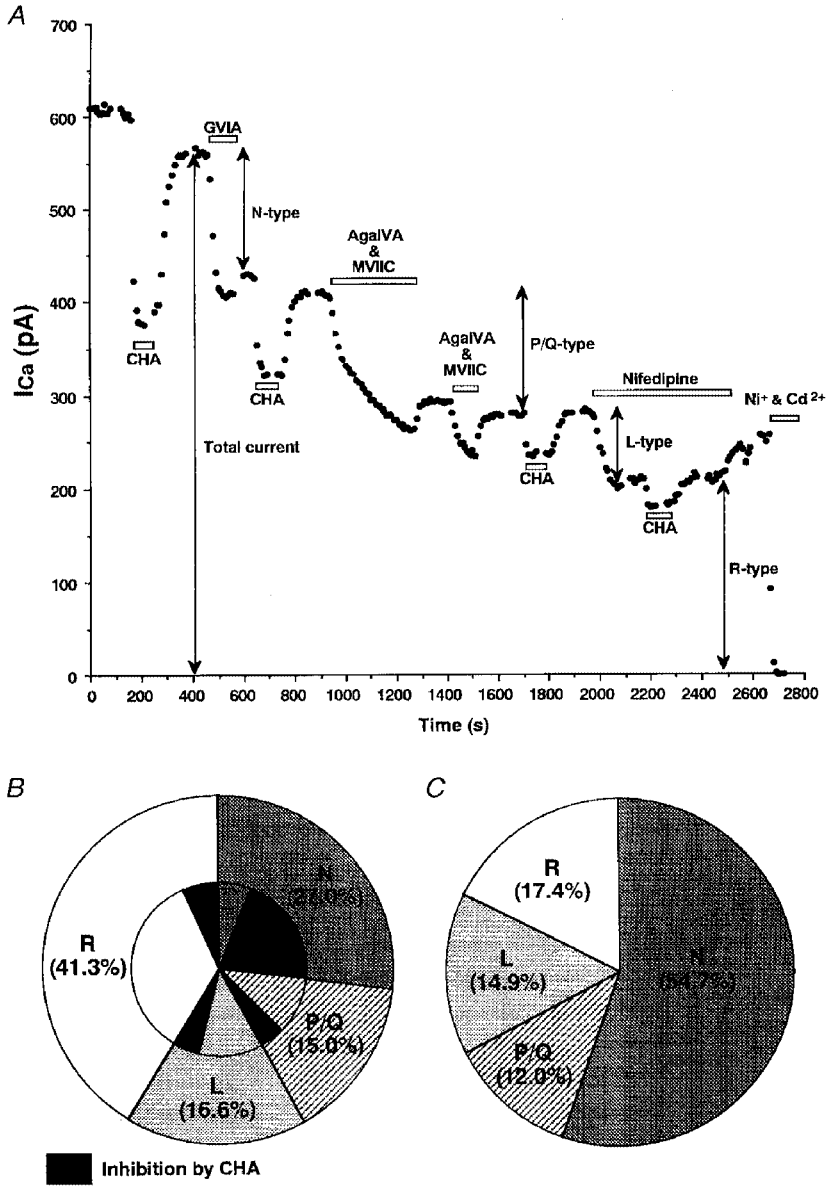

Figure 5. Analyses of VDCC subtypes contributing to CHA-induced I_{Ca} inhibition

A, a representative experiment illustrating the effect of 10^{-6} M CHA on I_{Ca} before and after application of various selective Ca^{2+} channel blockers. N-type Ca^{2+} current was the component irreversibly blocked by ω-CTx-GVIA (10^{-6} M; GVIA). P/Q-type Ca^{2+} current was the component irreversibly blocked by a combination of ω-Aga-IVA (10^{-7} M; AgaIVA) and ω-CTx-MVIIC (10^{-6} M; MVIIC). L-type Ca^{2+} current was the component reversibly blocked by nifedipine (10^{-5} M). The residual component insensitive to these drugs was regarded as R-type. *B*, summary of the distribution of high-voltage-activated Ca^{2+} channel subtypes (outer circle) and their fractional components which were sensitive to 10^{-6} M CHA (inner circle, black area) from four SON neurones. *C*, summary data for the relative proportion of each Ca^{2+} channel subtype that contributed to the total CHA-induced I_{Ca} inhibition.

Furukawa *et al.* 1998). In the present study, a prepulse to +150 mV for 100 ms reversed the majority of the adenosine-induced inhibition. In the presence of CHA, the I_{Ca} following such as a prepulse (C_2) was much larger than the current observed prior to the prepulse (C_1). In addition to the increased amplitude, the I_{Ca} following this prepulse displayed normal activation kinetics without the characteristic adenosine-induced 'kinetic slowing' (Fig. 6*A*). Similar results were obtained in all other SON neurones examined ($n = 6$).

The facilitation of I_{Ca} following this prepulse was investigated in both the absence and the presence of 10^{-6} M CHA (Fig. 6*B*). In the absence of CHA, the facilitation ratio was $1{\cdot}22 \pm 0{\cdot}04$ ($n = 6$). This facilitated current is thought to reflect tonic voltage-dependent inhibition of the VDCCs by G-protein $\beta\gamma$ subunits (Ikeda, 1996; Herlitze *et al.* 1996). Application of CHA significantly increased this facilitation ratio to $1{\cdot}75 \pm 0{\cdot}10$ ($n = 6$, $P < 0{\cdot}05$). These results indicate that G-proteins are involved in the inhibition of I_{Ca} by adenosine.

To investigate whether $G_{i/o}$ mediates adenosine-induced inhibition of I_{Ca} in SON neurones, the effects of dialysis with preactivated PTX (1 μg ml^{-1}) were examined. Pre-activated PTX was applied intracellularly (see Methods), because extracellular application of PTX requires too much time for the effects to appear and it was difficult to maintain good conditions for acutely dissociated neurones for such a long time. I_{Ca} was measured at times 0–20 min, 30–50 min and > 60 min after the membrane was ruptured. This time course was considered sufficient for pre-activated PTX to be dialysed into the neurone and to catalyse PTX-sensitive G-proteins. There were no significant changes in CHA-induced I_{Ca} inhibition, even more than 1 h after the cell membrane was ruptured (0–20 min, $37{\cdot}1 \pm 7{\cdot}0$%; 30–50 min, $37{\cdot}2 \pm 6{\cdot}4$%; 60 min, $33{\cdot}2 \pm 3{\cdot}0$%). In addition the degree of inhibition in the 0–20 min period was similar to that observed without PTX in the pipette (Fig. 4*B*2). This result indicates that the PTX resistant G-protein α subunit may mediate the CHA-induced inhibition of I_{Ca}.

Existence of G_z in SON neurones

We investigated the existence of G_z α subunit in the SON and the PVN by using immunohistochemistry. We observed $G_z\alpha$-like immunoreactivity (LI) throughout the SON and PVN (Fig. 7). This result provides the first demonstration that $G_z\alpha$ exists in the SON and PVN. $G_z\alpha$ LI was also found, at similar levels, in the cortex and hippocampus (data not shown), and these observations were consistent with those of a previous study using the same antiserum for $G_z\alpha$ (Hinton *et al.* 1990).

DISCUSSION

The present study provides the first direct evidence that adenosine A_1 receptors are functionally expressed in SON neurones and, when activated by adenosine, mediate inhibition of I_{Ca}. The present study also indicates the involvement of G-proteins in the signal transduction pathway underlying this effect.

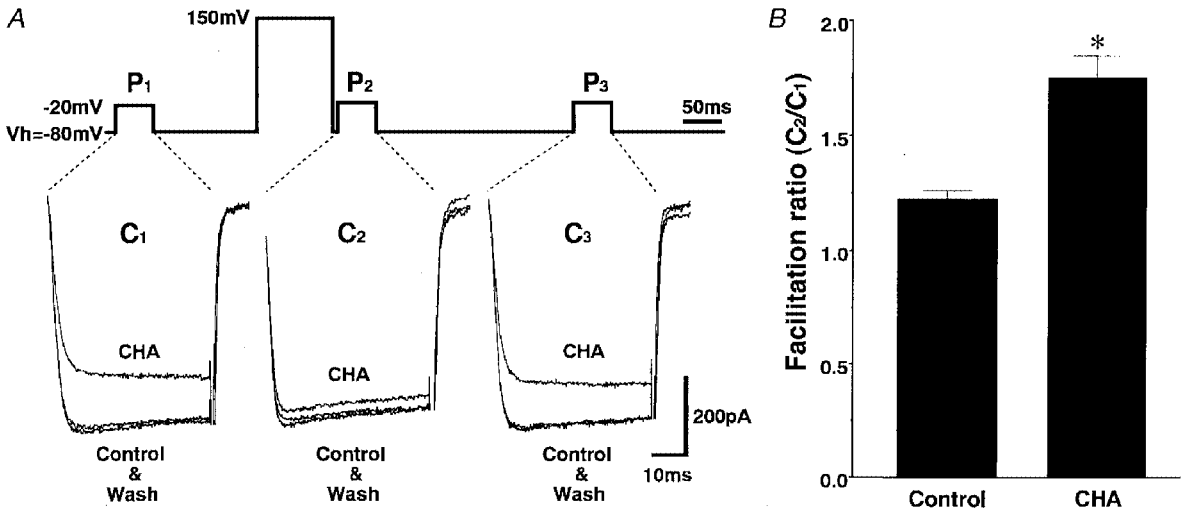

Figure 6. Effects of a depolarizing prepulse on CHA-induced I_{Ca} inhibition

A, three consecutive current traces in response to 50 ms test pulses from $V_h = -80$ to −20 mV. The middle test pulse (P2) was preceded by a 5 ms prepulse to +150 mV for 100 ms. The three traces in each panel correspond to before (Control), during and after (Wash) application of 10^{-6} M CHA. Most of the CHA-induced I_{Ca} inhibition was reversed by a depolarizing prepulse. *B*, summary of the change in the facilitation ratio by CHA. I_{Ca} amplitude between 3 and 8 ms was averaged and the facilitation ratio was calculated by dividing the C_2 current amplitude by the corresponding C_1 current amplitude. The facilitation ratio (C_2/C_1) was significantly greater in the presence of CHA than without CHA (control, $1{\cdot}22 \pm 0{\cdot}04$; CHA, $1{\cdot}75 \pm 0{\cdot}10$; $^*P < 0{\cdot}05$).

RT-PCR analysis of adenosine receptors in the SON

Classification of adenosine receptors is based on both their protein sequences and their affinity for a variety of ligands (Fredholm *et al.* 1994). Four subtypes of adenosine receptor have been cloned and pharmacologically characterized: A_1, A_{2a}, A_{2b} and A_3. Previous binding, immunohistochemical and *in situ* hybridization studies reported that the distribution of adenosine receptors was not high in rat brain hypothalamus. Only A_1 receptors were detected in the SON by *in situ* hybridization or immunohistochemistry (Reppert *et al.* 1991; Rivkees *et al.* 1995). Recently, however, Dixon and colleagues (Dixon *et al.* 1996) demonstrated the existence of all these subtypes of adenosine receptor in the hypothalamus by using RT-PCR, although their distribution within individual hypothalamic nuclei was not examined. In the present study, we have identified all these subtypes of adenosine receptor in the SON by using RT-PCR, although the expression level of the A_3 subtype was quite low.

Pharmacological analysis of adenosine receptor subtypes in SON neurones

Using reasonably selective agonists and antagonists, we have shown that the majority of the adenosine-induced inhibition of I_{Ca} in SON neurones was mediated by A_1 receptors. The evidence for this conclusion is as follows. Inhibition of I_{Ca} by adenosine or CHA was completely reversed by the selective A_1 receptor antagonist CPT. Because DMPX at 10^{-5} M has some affinity for the A_1 receptor (Seale *et al.* 1988), inhibition of I_{Ca} by adenosine or CHA was partially reversed by DMPX. While DPMA induced a small inhibition, it is likely that this was mediated via A_1 receptors as it was reversed by CPT. In addition, A_2 receptors have been reported to enhance I_{Ca} in other preparations (Mogul *et al.* 1993). Although the exact affinity of APNEA for each adenosine receptor subtype is still unclear, it has been reported that APNEA also has some affinity for the A_1 receptor (Armstrong & Ganote, 1994). The finding that APNEA inhibited I_{Ca} and that this was reversed by a selective A_1 receptor antagonist supports this suggestion.

VDCCs in the SON

VDCCs are characterized by both their pharmacological characteristics and the molecular identity of their α_1 subunits. In the SON neurones, five different high-voltage-activated (HVA) Ca^{2+} channels have been identified to date on the basis of pharmacology: L-, N-, P-, Q- and R-type (Fisher & Bourque, 1995; Foehring & Armstrong, 1996). Using specific Ca^{2+} channel blockers, we investigated their contribution to the total I_{Ca} in SON neurones.

The proportion of R-type I_{Ca} in the present study was larger (41 % of total I_{Ca}) than reported in previous studies (Fisher & Bourque, 1995; Foehring & Armstrong, 1996;

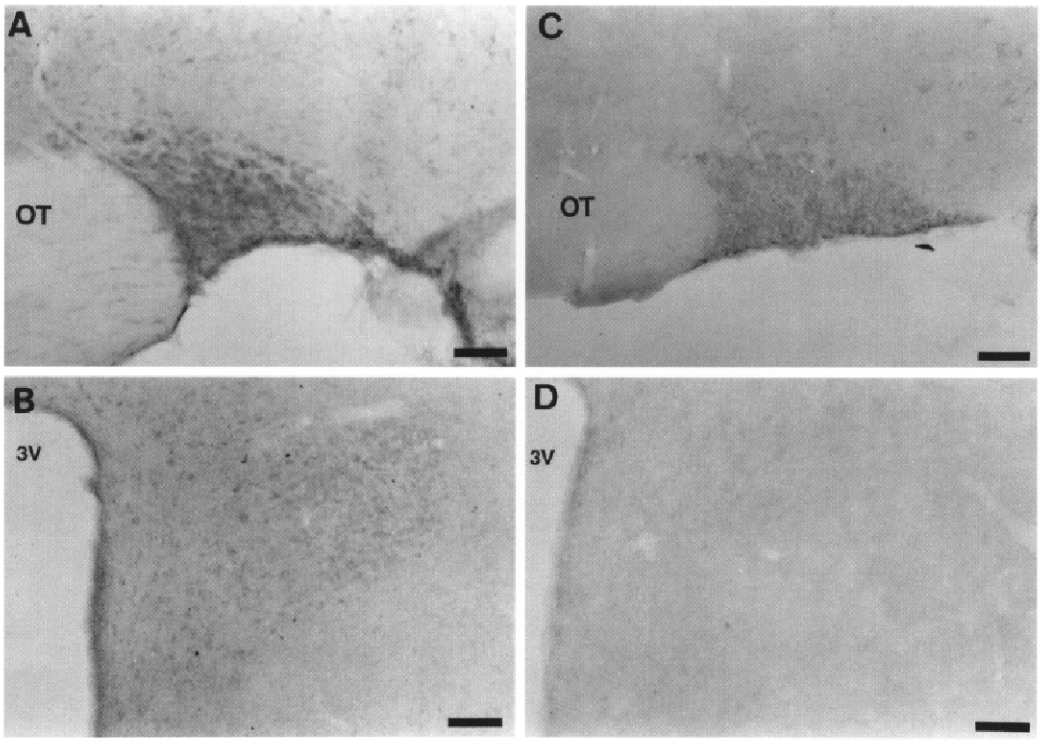

Figure 7. $G_z\alpha$-like immunoreactivity in the rat SON

Light micrograph illustrating $G_z\alpha$-like immunoreactivity in a coronal section of the SON (*A*) and PVN (*B*). The staining is found in the perikarya of SON neurones and PVN neurones. This positive staining was abolished by preincubation with $G_z\alpha$ (10^{-4} M) (*C* and *D*). OT, optic tract; 3V, third ventricle. Scale bars, 50 μm.

Harayama *et al.* 1998; Soldo & Moises, 1998) although this result is in good agreement with the observation that there is a large amount of mRNA for R-type channel α subunit (α_{1E}) in the SON (Soong *et al.* 1993). A developmental difference in the relative amount of VDCCs may be one of the reasons for these differences (Widmer *et al.* 1997). Complex factors such as different strains of rats and drug application protocol might also have contributed to the difference in proportion of HVA Ca^{2+} channel subtypes.

In the present study, the peak current appeared at a relatively low potential (−20 mV) when compared with these previous studies, where the peak current appeared at around −10 mV in adult rats (Fisher & Bourque, 1995; Foehring & Armstrong, 1996) and was at 0 mV in infant rats (Harayama *et al.* 1998; Soldo & Moises, 1998). Because R-type Ca^{2+} channels encoded by α_{1E} show a relatively lower voltage threshold and peak activation than any of the other HVA Ca^{2+} channels (Chin *et al.* 1992; Soong *et al.* 1993; Dunlap *et al.* 1995), the negative shift of the current–voltage relationship in the present study may be caused by a large proportion of R-type I_{Ca}.

The Ca^{2+} channel subtype susceptible to inhibition by A_1 agonist

In the present study, by using inhibitors of VDCCs, distinct subtypes of HVA I_{Ca} were identified in the somata of SON neurones. Although all subtypes of HVA I_{Ca} were inhibited by the A_1 agonist CHA, the relative contribution of each subtype to the total CHA-induced inhibition differed. N-type Ca^{2+} channels made the largest contribution to the CHA-induced inhibition of I_{Ca}. Although adenosine inhibits different subtypes of VDCC in different neuronal preparations, the most common target seems to be N-type VDCCs. For example, adenosine inhibits N-type I_{Ca} in the hippocampus, brainstem and superior cervical ganglion (Mogul *et al.* 1993; Zhu & Ikeda, 1993; Umemiya & Berger, 1994; Fleming & Mogul, 1997). Although the specific physiological role of each subtype is not clear in the SON, it has been reported that L- or N-type channel blockers significantly reduce depolarizing afterpotentials (DAPs) (Li & Hatton, 1997). These DAPs are important in the generation and/or maintenance of the phasic firing pattern in vasopressin-secreting neurones. Thus, N-type I_{Ca} in the somata of SON neurones may make a significant contribution to the regulation of hormone release from the neurohypophysis.

Signal transduction pathway for the inhibition of VDCCs by adenosine

Adenosine-induced inhibition occurred within a few seconds and was associated with a kinetic slowing of I_{Ca} activation. In addition, the inhibition was reversed by a large depolarizing prepulse. These effects suggest that the inhibition is mediated through G-proteins via a membrane-delimited pathway without the involvement of soluble intracellular second messengers (Ikeda, 1996; Herlitze *et al.* 1996; Furukawa *et al.* 1998). In the membrane-delimited pathway, it has been suggested that there are two direct interaction pathways between G-protein subunits and VDCCs. One is a voltage-independent pathway via the G-protein α subunit and the other is a voltage-dependent pathway via the G-protein $\beta\gamma$ subunit. In the case of SON neurones, the majority of the CHA (adenosine)-induced inhibition was reversed by a depolarizing prepulse suggesting that the inhibition of I_{Ca} by adenosine is mainly mediated by $G\beta\gamma$. CHA (adenosine), however, inhibited all subtypes of HVA VDCCs in the present study (Fig. 5) and a depolarizing prepulse did not completely reverse this adenosine-induced inhibition. Recently, it has been suggested that agonist-induced inhibition of N-, P/Q- and R-type VDCCs is reversed by a large depolarizing prepulse, but inhibition of L-type VDCCs is not (Zhang *et al.* 1996; Qin *et al.* 1997; Furukawa *et al.* 1998). The residual component, which was not reversed by a prepulse, might therefore be L-type and/or parts of other subtypes of VDCC, which are mediated by $G\alpha$ in a voltage-independent manner.

PTX resistance of SON neurones

It is widely accepted that adenosine A_1 receptors couple to $G_{i/o}$ proteins, which are sensitive to PTX. In the present study, however, PTX did not affect the CHA (adenosine)-induced inhibition of I_{Ca}. The technique used to intracellularly apply PTX has previously been shown to be effective in significantly diminishing 5-HT-induced inhibition of Ba^{2+} currents in melanotrophs (Noguchi & Yamashita, 1999). The dose used in the present study (1 μg ml^{-1}) was considered to be sufficient to completely ribosylate $G_{i/o}$ proteins in SON neurones. Similar PTX-resistant phenomena have been reported in SON and other hypothalamic neurones. In slice preparations of adult rat SON, pretreatment with PTX did not affect the baclofen-induced depression of IPSCs under the same conditions in which PTX blocked the postsynaptic $GABA_B$ response in neurones of the lateral parabrachial nucleus (Mouginot *et al.* 1998). In cultured hypothalamic suprachiasmatic nucleus neurones, it has been reported that baclofen-induced inhibition of postsynaptic VDCCs is not fully blocked after PTX pretreatment (Chen & van den Pol, 1998). In our previous study, baclofen-induced inhibition of I_{Ca} in dissociated SON neurones from infant rats also seemed to be relatively resistant to PTX (Harayama *et al.* 1998). These reports suggest that in hypothalamic neurones, including SON neurones, inhibitory G-proteins might be unusually resistant to PTX. Using *in situ* hybridization histochemistry, the distribution of the gene expression of G-protein subtypes in the CNS including the SON has been reported. G_s mRNA was strongly expressed in the SON, whereas $G_{i/o}$ mRNA could not be detected in the SON (Noguchi & Yamashita, 1999). These reports support the possibility that the level of $G_{i/o}$ protein in SON neurones is insufficient to mediate A_1 receptor coupling and subsequent I_{Ca} inhibition. To address this issue, we investigated the existence of $G_z\alpha$ in the SON by using immunohistochemistry. The result

indicates that there were G_z α subunits in SON neurones. $G_z\alpha$ is a member of the $G_{i/o}$ protein superfamily but is resistant to PTX, and recently it has been reported that $G_z\alpha$ mediates agonist-induced inhibition of VDCCs (Jeong & Ikeda, 1998; Furukawa *et al.* 1998). At present there are no tools available to elucidate signal pathways mediated by $G_z\alpha$ in native cells, thus we could not provide direct evidence that $G_z\alpha$ mediated the adenosine-induced inhibition of I_{Ca} in SON neurones. Nevertheless, the present results are consistent with an involvement of $G_z\alpha$ in mediating the adenosine-induced inhibition of I_{Ca}. Further experiments are needed to more directly determine which subtypes of G-protein mediate the inhibition of I_{Ca} by adenosine.

Physiological implications of the inhibition of VDCCs by adenosine

We observed that adenosine inhibited I_{Ca} in all the recorded cells, which were dissociated randomly from various areas of the SON. This suggests that Ca^{2+} currents in both vasopressin- and oxytocin-secreting neurones were modulated by adenosine.

In the hypothalamo-neurohypophysial system, the amount of hormone release from the axon terminals is highly dependent on the electrical activity of SON neurones (Bourque, 1991; Leng & Brown, 1997). Ca^{2+} entry through VDCCs during action potentials makes an important contribution to this electrical activity. More specifically, Ca^{2+} influx through VDCCs is required for action potential broadening in response to different firing frequencies, which leads to a facilitation of hormone release in both oxytocin and vasopressin neurones (Bourque & Renaud, 1985). In addition, Ca^{2+} influx is essential for action potential DAPs which summate potentials which then initiate phasic burst firing and vasopressin secretion (Bourque, 1986). Furthermore, the subsequent activation of Ca^{2+}-dependent potassium conductances also contributes to the pattern and rate of firing in both oxytocin and vasopressin neurones (Kirkpatrick & Bourque, 1996). In SON neurones, protein phosphorylation, enzyme activity, gene expression and somatodendritic release of both oxytocin and vasopressin are also thought to be Ca^{2+}-dependent processes. Ca^{2+} influx through VDCCs may be important for these events. Hence the inhibition of VDCCs is an important cellular mechanism whereby adenosine may contribute to the electrical activity and neurosecretion in SON neurones.

We revealed that functional adenosine receptors exist in post-synaptic membranes of SON neurones and that adenosine acts as inhibitory modulator. However, in physiological situations, where does the adenosine come from?

Recently, Oliet & Poulain (1999) revealed that in the SON, endogenous adenosine is released into the extracellular space in response to electrical field stimulation and acts as an inhibitor of neurotransmitter release from presynaptic terminals projecting to SON magnocellular neurones. While the specific origin of this endogenous adenosine is not clear, there are two general possibilities.

One is intracellular adenosine that is formed from the breakdown of ATP. In general, when cellular activity increases, intracellular ATP is metabolized to adenosine which can be directly released into the extracellular space via transport processes present in various types of cell. The possible sites that could release adenosine in the SON are neuronal terminals, glial cells and SON neurones themselves (Oliet & Poulain, 1999). If adenosine is released from the SON neurones themselves, adenosine may mediate an activity-dependent negative feedback action.

Another possible source of endogenous adenosine is from the breakdown of neuronally released ATP by ecto-nucleotidases in the extracellular space. For instance, noradrenergic fibres, which project to the SON (Pittman, 1999) and SON magnocellular neurones themselves both contain ATP in their synaptic vesicles (Troadec *et al.* 1998; Pittman, 1999). The released ATP can be metabolized to adenosine by ecto-ATPase in the extracellular synaptic space in the SON. In this case, adenosine may act to terminate the excitatory effect of ATP.

In conclusion, the present study has demonstrated that functional A_1 adenosine receptors are present in the postsynaptic membrane of SON magnocellular neurones where they mediate inhibition of VDCCs, in particular the N-type channel, via PTX-resistant, membrane-delimited, G-proteins.

Andrew, R. D. (1987). Endogenous bursting by rat supraoptic neuroendocrine cells is calcium dependent. *Journal of Physiology* **384**, 451–465.

Armstrong, S. & Ganote, C. E. (1994). Adenosine receptor specificity in preconditioning of isolated rabbit cardiomyocytes: evidence of A_3 receptor involvement. *Cardiovascular Research* **28**,1049–1056.

Birnbaumer, L., Campbell, K. P., Catterall, W. A., Harpold, M. M., Hofmann, F., Horne, W. A., Mori, Y., Schwartz, A., Suntch, T. P. & Tsien, R. W. (1994). The naming of voltage-gated calcium channels. *Neuron* **13**, 505–506.

Bourque, C. W. (1986). Calcium-dependent spike after-current induces burst firing in magnocellular neurosecretory cells. *Neuroscience Letters* **70**, 204–209.

Bourque, C. W. (1991). Activity-dependent modulation of nerve terminal excitation in a mammalian peptidergic system. *Trends in Neurosciences* **14**, 29–30.

Bourque, C. W. & Renaud, L. P. (1985). Activity dependence of action potential duration in rat supraoptic neurosecretory neurones recorded *in vitro*. *Journal of Physiology* **363**, 429–439.

Brann, D. W. (1995). Glutamate: a major excitatory transmitter in neuroendocrine regulation. *Neuroendocrinology* **61**, 213–225.

Chen, G. & van den Pol, A. N. (1998). Presynaptic $GABA_B$ autoreceptor modulation of P/Q-type calcium channels and GABA release in rat suprachiasmatic nucleus neurons. *Journal of Neuroscience* **18**, 1913–1922.

Chin, H., Smith, M. A., Kim, H. L. & Kim, H. (1992). Expression of dihydropyridine-sensitive brain calcium channels in the rat central nervous system. *FEBS Letters* **299**, 69–74.

de Mendonća, A. & Ribeiro, J. A. (1994). Endogenous adenosine modulates long-term potentiation in the hippocampus. *Neuroscience* **62**, 385–390.

Dixon, A. K., Gubitz, A. K., Sirinathsinghji, D. J., Richardson, P. J. & Freeman, T. C. (1996). Tissue distribution of adenosine receptor mRNAs in the rat. *British Journal of Pharmacology* **118**, 1461–1468.

Dragunow, M. (1988). Purinergic mechanisms in epilepsy. *Progress in Neurobiology* **31**, 85–108.

Dragunow, M. & Faull, R. L. (1988). Neuroprotective effects of adenosine. *Trends in Pharmacological Sciences* **9**, 193–194.

Dunlap, K., Luebke, J. I. & Turner, T. J. (1995). Exocytotic Ca^{2+} channels in mammalian central neurons. *Trends in Neurosciences* **18**, 89–98.

Fisher, T. E. & Bourque, C. W. (1995). Voltage-gated calcium currents in the magnocellular neurosecretory cells of the rat supraoptic nucleus. *Journal of Physiology* **486**, 571–580.

Fleming, K. M. & Mogul, D. J. (1997). Adenosine A_3 receptors potentiate hippocampal calcium current by a PKA-dependent/PKC-independent pathway. *Neuropharmacology* **36**, 353–362.

Foehring, R. C. & Armstrong, W. E. (1996). Pharmacological dissection of high-voltage-activated Ca^{2+} current types in acutely dissociated rat supraoptic magnocellular neurons. *Journal of Neurophysiology* **76**, 977–983.

Fredholm, B. B., Abbracchio, M. P., Burnstock, G., Daly, J. W., Harden, T. K., Jacobson, K. A., Leff, P. & Williams, M. (1994). Nomenclature and classification of purinoceptors. *Pharmacological Reviews* **46**, 143–156.

Fredholm, B. B. & Dunwiddie, T. V. (1988). How does adenosine inhibit transmitter release? *Trends in Pharmacological Sciences* **9**, 130–134.

Furukawa, T., Miura, R., Mori, Y., Strobeck, M., Suzuki, K., Ogihara, Y., Asano, T., Morishita, R., Hashii, M., Higashida, H., Yoshii, M. & Nukada, T. (1998). Differential interactions of the C terminus and the cytoplasmic I-II loop of neuronal Ca^{2+} channels with G-protein α and $\beta\gamma$ subunits. II. Evidence for direct binding. *Journal of Biological Chemistry* **273**, 17595–17603.

Harayama, N., Shibuya, I., Tanaka, K., Kabashima, N., Ueta, Y. & Yamashita, H. (1998). Inhibition of N- and P/Q-type calcium channels by postsynaptic $GABA_B$ receptor activation in rat supraoptic neurones. *Journal of Physiology* **509**, 371–383.

Hatton, G. I. (1990). Emerging concepts of structure-function dynamics in adult brain: the hypothalamo-neurohypophysial system. *Progress in Neurobiology* **34**, 437–504.

Herlitze, S., Garcia, D. E., Mackie, K., Hille, B., Scheuer, T. & Catterall, W. A. (1996). Modulation of Ca^{2+} channels by G-protein $\beta\gamma$ subunits. *Nature* **380**, 258–262.

Hinton, D. R., Blanks, J., Fong, H. K., Casey, P. J., Hildebrandt, E. & Simons, M. I. (1990). Novel localization of a G protein, Gz-α, in neurons of brain and retina. *Journal of Neuroscience* **10**, 2763–2770.

Ikeda, S. R. (1996). Voltage-dependent modulation of N-type calcium channels by G-protein $\beta\gamma$ subunits. *Nature* **380**, 255–258.

Jeong, S. W. & Ikeda, S. R. (1998). G protein alpha subunit Gαz couples neurotransmitter receptors to ion channels in sympathetic neurons. *Neuron* **21**, 1201–1212.

Kakehata, S., Nakagawa, T., Takasaka, T. & Akaike, N. (1993). Cellular mechanism of acetylcholine-induced response in dissociated outer hair cells of guinea-pig cochlea. *Journal of Physiology* **463**, 227–244.

Kirkpatrick, K. & Bourque, C. W. (1996). Activity dependence and functional role of the apamin-sensitive K^+ current in rat supraoptic neurones *in vitro*. *Journal of Physiology* **494**, 389–398.

Leng, G. & Brown, D. (1997). The origins and significance of pulsatility in hormone secretion from the pituitary. *Journal of Neuroendocrinolgy* **9**, 493–513.

Li, Z. & Hatton, G. I. (1997). Ca^{2+} release from internal stores: role in generating depolarizing after-potentials in rat supraoptic neurones. *Journal of Physiology* **498**, 339–350.

Mogul, D. J., Adams, M. E. & Fox, A. P. (1993). Differential activation of adenosine receptors decreases N-type but potentiates P-type Ca^{2+} current in hippocampal CA3 neurons. *Neuron* **10**, 327–334.

Mouginot, D., Kombian, S. B. & Pittman, Q. J. (1998). Activation of presynaptic $GABA_B$ receptors inhibits evoked IPSCs in rat magnocellular neurons *in vitro*. *Journal of Neurophysiology* **79**, 1508–1517.

Noguchi, J. & Yamashita, H. (1999). Baclofen inhibits postsynaptic voltage-dependent calcium currents of supraoptic nucleus neurons isolated from young rats. *Biomedical Research* **20**, 239–247.

Oliet, S. H. & Bourque, C. W. (1992). Properties of supraoptic magnocellular neurones isolated from the adult rat. *Journal of Physiology* **455**, 291–306.

Oliet, S. H. R. & Poulain, D. A. (1999). Adenosine-induced presynaptic inhibition of IPSCs and EPSCs in rat hypothalamic supraoptic nucleus neurones. *Journal of Physiology* **520**, 815–825.

Palmer, T. M. & Stiles, G. L. (1995). Adenosine receptors *Neuropharmacology* **34**, 683–694.

Pittman, Q. J. (1999). The action is at the terminal. *Journal of Physiology* **520**, 629.

Qin, N., Platano, D., Olcese, R., Stefani, E. & Birnbaumer, L. (1997). Direct interaction of G$\beta\gamma$ with a C-terminal G$\beta\gamma$-binding domain of the Ca^{2+} channel alpha1 subunit is responsible for channel inhibition by G protein-coupled receptors. *Proceedings of the National Academy of Sciences of the USA* **94**, 8866–8871.

Rainnie, D. G., Grunze, H. C., McCarley, R. W. & Greene, R. W. (1994). Adenosine inhibition of mesopontine cholinergic neurons: implications for EEG arousal. *Science* **263**, 689–692.

Reppert, S. M., Weaver, D. R., Stehle, J. H. & Rivkees, S. A. (1991). Molecular cloning and characterization of a rat A_1-adenosine receptor that is widely expressed in brain and spinal cord. *Molecular Endocrinology* **5**, 1037–1048.

Rivkees, S. A., Price, S. L. & Zhou, F. C. (1995). Immunohistochemical detection of A_1 adenosine receptors in rat brain with emphasis on localization in the hippocampal formation, cerebral cortex, cerebellum, and basal ganglia. *Brain Research* **677**, 193–203.

Seale, T. W., Abla, K. A., Shamim, M. T., Carney, J. M. & Daly, J. W. (1988). 3,7-Dimethyl-1-propargylxanthine: a potent and selective *in vivo* antagonist of adenosine analogs. *Life Sciences* **43**, 1671–1684.

Shibuya, I., Tanaka, K., Hattori, Y., Uezono, Y., Harayama, N., Noguchi, J., Ueta, Y., Izumi, F. & Yamashita, H. (1999). Evidence that multiple P2X purinoceptors are functionally expressed in rat supraoptic neurones. *Journal of Physiology* **514**, 351–367.

Soldo, B. L. & Moises, H. C. (1998). μ-Opioid receptor activation inhibits N- and P-type Ca^{2+} channel currents in magnocellular neurones of the rat supraoptic nucleus. *Journal of Physiology* **513**, 787–804.

Soong, T. W., Stea, A., Hodson, C. D., Dubel, S. J., Vincent, S. R. & Snutch, T. P. (1993). Structure and functional expression of a member of the low voltage-activated calcium channel family. *Science* **260**, 1133–1136.

Troadec, J.-D., Thirion, S., Nicaise, G., Lemos, J. R. & Dayanithi, G. (1998). ATP-evoked increases in $[Ca^{2+}]_i$ and peptide release from rat isolated neurohypophysial terminals via a P_{2X2} purinoceptor. *Journal of Physiology* **511**, 89–103.

Umemiya, M. & Berger, A. J. (1994). Activation of adenosine A_1 and A_2 receptors differentially modulates calcium channels and glycinergic synaptic transmission in rat brainstem. *Neuron* **13**, 1439–1446.

Widmer, H., Amerdeil, H., Fontanaud, P. & Desarmenien, M. G. (1997). Postnatal maturation of rat hypothalamoneurohypophysial neurons: evidence for a developmental decrease in calcium entry during action potentials. *Journal of Neurophysiology* **77**, 260–271.

Zhang, J. F., Ellinor, P. T., Aldrich, R. W. & Tsien, R. W. (1996). Multiple structural elements in voltage-dependent Ca^{2+} channels support their inhibition by G proteins. *Neuron* **17**, 991–1003.

Zhu, Y. & Ikeda, S. R. (1993). Adenosine modulates voltage-gated Ca^{2+} channels in adult rat sympathetic neurons. *Journal of Neurophysiology* **70**, 610–620.

Acknowledgements

This study was supported in part by grants from the Ministry of Education, Science, Sports and Culture, Japan (to H.Y., nos 10470019 and 10218210), a research grant from the Ministry of Health and Welfare, and the Salt Science Research Foundation. We thank Dr Andrew Moorhouse (School of Physiology and Pharmacology, The University of New South Wales, Australia) and Dr Toshihisa Nagatomo (2nd Department of Internal Medicine, University of Occupational and Environmental Health) for helpful comments on this manuscript, Dr Yasuhito Uezono (Department of Pharmacology, Miyazaki Medical College, Japan) for technical advice and Ms Yuko Hara for technical assistance.

Corresponding author

J. Noguchi: Department of Physiology, School of Medicine, University of Occupational and Environmental Health, 1-1 Iseigaoka, Yahatanishi-ku, Kitakyushu 807-8555, Japan.

Email: n-jun@med.uoeh-u.ac.jp

Author's present address

H. Yamashita: Kyurin Medical Laboratory, 27-25 Morishita Yahatanishi-ku, Kitakyshu 806-0046, Japan.